

# **Attenuation and Rain Rate Estimation from Airborne and Combined Airborne and Ground-Based Millimeter Cloud Radar Measurements**

*L. Li, S. M. Sekelsky, G. A. Sadowy, and S. C. Reising  
Microwave Remote Sensing Laboratory  
University of Massachusetts  
Amherst, Massachusetts*

*S. L. Durden, S. J. Dindardo, and F. K. Li  
Jet Propulsion Laboratory  
California Institute of Technology  
Pasadena, California*

*A. C. Huffman III and G. L. Stephens  
Department of Atmospheric Science  
Colorado State University  
Fort Collins, Colorado*

## **Introduction**

Millimeter-wave radars offer significant advantages over low frequency radars. Because of the high scattering efficiency and short wavelength at millimeter-wave frequencies, compact and low-power radars can be built for use in portable systems, especially for airborne and spaceborne applications. On the other hand, attenuation due to the atmosphere, clouds, and precipitation increase considerably at millimeter-wave frequencies. Calculation of reflectivity under attenuating conditions is not trivial.

In June 1998, The Airborne Cloud Radar (ACR) (Sadowy et al. 1997), jointly developed by the University of Massachusetts (UMass) and the National Aeronautics and Space Administration's (NASA's) Jet Propulsion Laboratory, was installed on the NASA DC-8 aircraft and deployed along with the ground-based UMass Cloud Profiling Radar System (CPRS) (Sekelsky 1996). The measurements were conducted initially at the Department of Energy's Cloud and Radiation Testbed (CART) site in Lamont, Oklahoma, and subsequently in New Iberia, Louisiana. The objective of these coordinated measurements is to intercompare cloud radar calibrations and to better characterize clouds and precipitation by comparing the propagation of the upward-looking and downward-looking millimeter-wave radar signals. Cloud and precipitation data were collected during ACR overflights of CPRS and during ACR flights over the ocean. Two algorithms that retrieve vertical profiles of attenuation and rain rate are presented. The first combines collocated airborne and ground-based radar reflectivity profiles and requires no assumptions about the cloud and precipitation microphysics. The second uses nadir-pointing airborne radar reflectivity profiles measured over the ocean. The latter algorithm also uses the ocean surface return as a reference to determine total attenuation for the column

of atmosphere measured. This paper describes the algorithm and results derived from the data collected at New Iberia, Louisiana. The radar calibration effort is discussed by another paper (Sekelsky et al. 1999) in this proceedings.

## Dual Radar Measurement Algorithm

For radar operating at attenuating frequencies, the true reflectivity  $Z_e^t(h)$  is related to the measured reflectivity  $Z_e^m(h)$  in dB by

$$Z_e^t(h) = Z_e^m(h) + 2 \int_0^h K_e(r) dr, \quad (1)$$

where  $h$  is the range height and  $K_e = K_a + K_p + K_c$ , is the total attenuation rate (dB/km) due to atmospheric gases ( $K_a$ ), precipitation ( $K_p$ ), and clouds ( $K_c$ ).

One method for retrieving attenuation uses simultaneous measurements from two radars, one above and one below the clouds and precipitation. In the following equations,  $Z_{e,u}^m$  and  $Z_{e,d}^m$  represent the equivalent reflectivity measured by ground-based upward-looking radar and by airborne downward-looking radar respectively.  $Z_e^t$  is the unattenuated equivalent reflectivity. We use  $Z_e$  to denote the possibility of Mie scattering, which is frequently observed at 95 GHz. For the upward-looking radar we have:

$$Z_e^t(h) = Z_{e,u}^m(h) + 2 \int_0^h K_e(r) dr + C, \quad (2)$$

where  $C$  is the radome attenuation caused by water laying on the antenna. Boundary conditions are found from the radar measurements at cloud top and at the surface. These are given as  $Z_e^t(H) = Z_{e,u}^m(H) + A + C$  and  $Z_e^t(0) = Z_{e,u}^m(0) + C$ , respectively.  $A = 2 \int_0^H K_e(r) dr$  is the two-way path integrated attenuation (PIA), and  $H$  is the height of the cloud top. For the downward-looking radar we have:

$$Z_e^t(h) = Z_{e,d}^m(h) + 2 \int_h^H K_e(r) dr. \quad (3)$$

Cloud top and surface measurements are given as  $Z_e^t(H) = Z_{e,d}^m(H)$  and  $Z_e^t(0) = Z_{e,d}^m(0) + A$ .  $A$  and  $C$  can be determined by using these boundary conditions. The unattenuated reflectivity then is written as:

$$Z_e^t(h) = (Z_{e,u}^m(h) + Z_{e,d}^m(h) + A + C) / 2. \quad (4)$$

This dual radar measurement has unique advantages. First, reflectivity and attenuation can be retrieved at each range height by combining the upward-looking and downward-looking radar profiles. Second, a priori knowledge about the attenuation from clouds, the atmosphere and precipitation is not required. This significantly reduces the uncertainty in the retrieved reflectivity.

Although rain rate estimation is not the primary goal of this analysis, rain rate is obtained along with the attenuation calculation. This can be done by using different approaches, which relate  $Z_e^t$ , radar signal attenuation rate due to rain  $K_p$  and rainfall rate  $R$ . One way to find the internal relations between these parameters is using their original definitions for specific raindrop size distribution (Doviak and Zrnich 1993). The other approach is using power laws  $Z_e^t = a R^b$  and  $K_p = \alpha R^\beta$  under approximations.

## Single Radar Measurement Algorithm

Based on the relations between  $Z_e^t$ ,  $K_p$ , and  $R$ , reflectivity can also be retrieved from single radar measurements. By using power law relations, Hitschfeld and Bordan (HB) (1954) showed that Eq. (1) can be rewritten as a first-order differential equation with an analytical solution.  $Z_e^t$ ,  $K_p$ , and  $R$  can be estimated from measured reflectivity. However, errors in the power relations can cause considerable errors in the retrieved profiles or even divergence at far ranges. One way to overcome this problem is to use path integrated attenuation (PIA) as a constraint. PIA can be derived from measurements by a second radar or from the surface reference technique (SRT) (Meneghini et al. 1983), in which the path attenuation is determined by comparing ocean surface return from a precipitating region and precipitation free region.

## Radar Measurements and Retrieval Results

The dual radar measurement case is illustrated using measurements from the coastal area of southern Louisiana. Figure 1 shows the airborne and ground-based radar reflectivity profiles when the DC-8 passed over the ground-based CPRS system. Averaging times are selected to maximize sample volume overlaps for the two radars. Atmospheric attenuation is derived from radiosonde data and the Liebe (1985) model of water vapor absorption. The solid curve is the retrieved reflectivity. Figure 2 plots the two-way cumulative attenuation due to rain, which is calculated by combining the upward-looking and downward-looking radar reflectivity and removing the atmospheric gas attenuation. In this overpass case, the total two-way PIA due to the atmosphere is approximately 7.7 dB, while the two-way PIA due to rain is approximately 21 dB. Precipitation below 4.5 km produces a two-way attenuation rate of 4.8 dB/km. The ice cloud (above 5 km) has a two-way attenuation rate of 0.38 dB/km.

Rain rate,  $R$ , is retrieved from  $Z_e^t$  and  $K_p$  using different drop size distribution (DSD) and power law relationships. The HB algorithm is also applied to individual radar measurement using data from the second radar to estimate PIA. The reflectivity and rain rate retrieved using the HB algorithm with Marshall-Palmer DSD is shown in Figure 3. Figure 4 shows results retrieved using the HB algorithm and power law relations with coefficients given by Haddad et al (1997). Reflectivity retrieved by combining upward- and downward-looking profiles is also plotted for comparison.

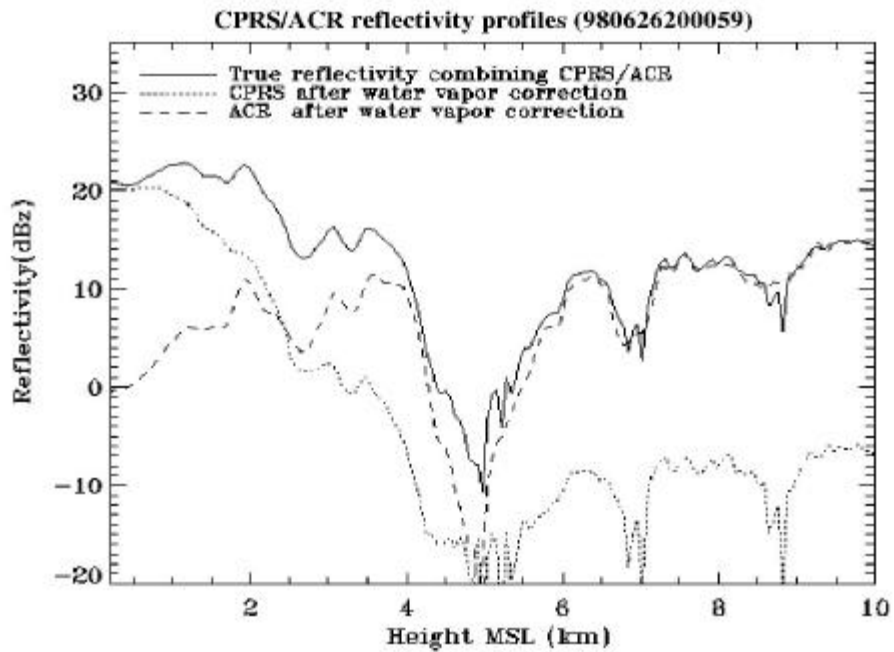


**Figure 1.** CPRS and ACR reflectivity profiles when the aircraft passed over the ground-based radar. The solid line is the reflectivity retrieved by combining CPRS and ACR measurements.

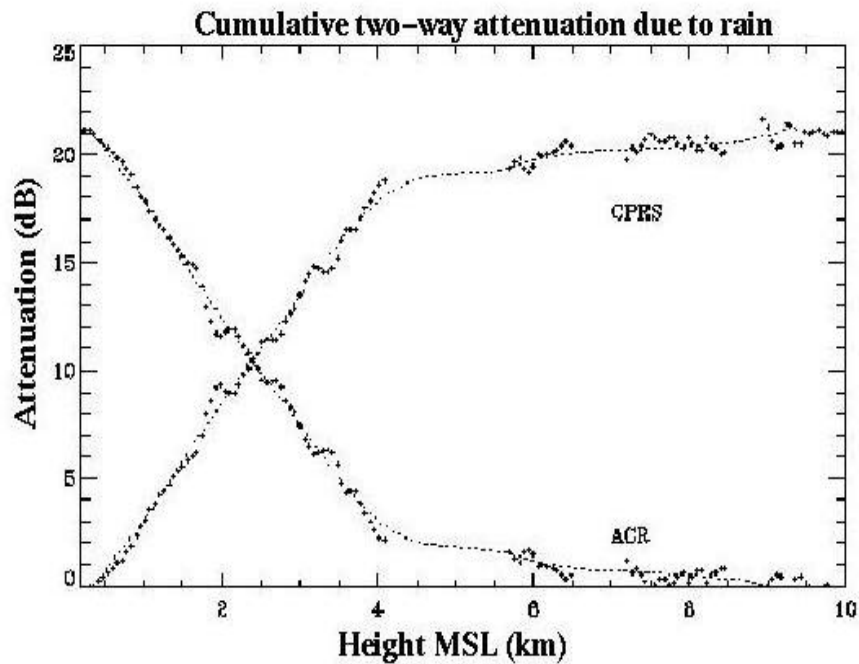


**Figure 2.** Two-way cumulative attenuation due to rain. The attenuation rate is 4.8 dB/km in the precipitation region and 0.38 dB/km in the ice clouds.

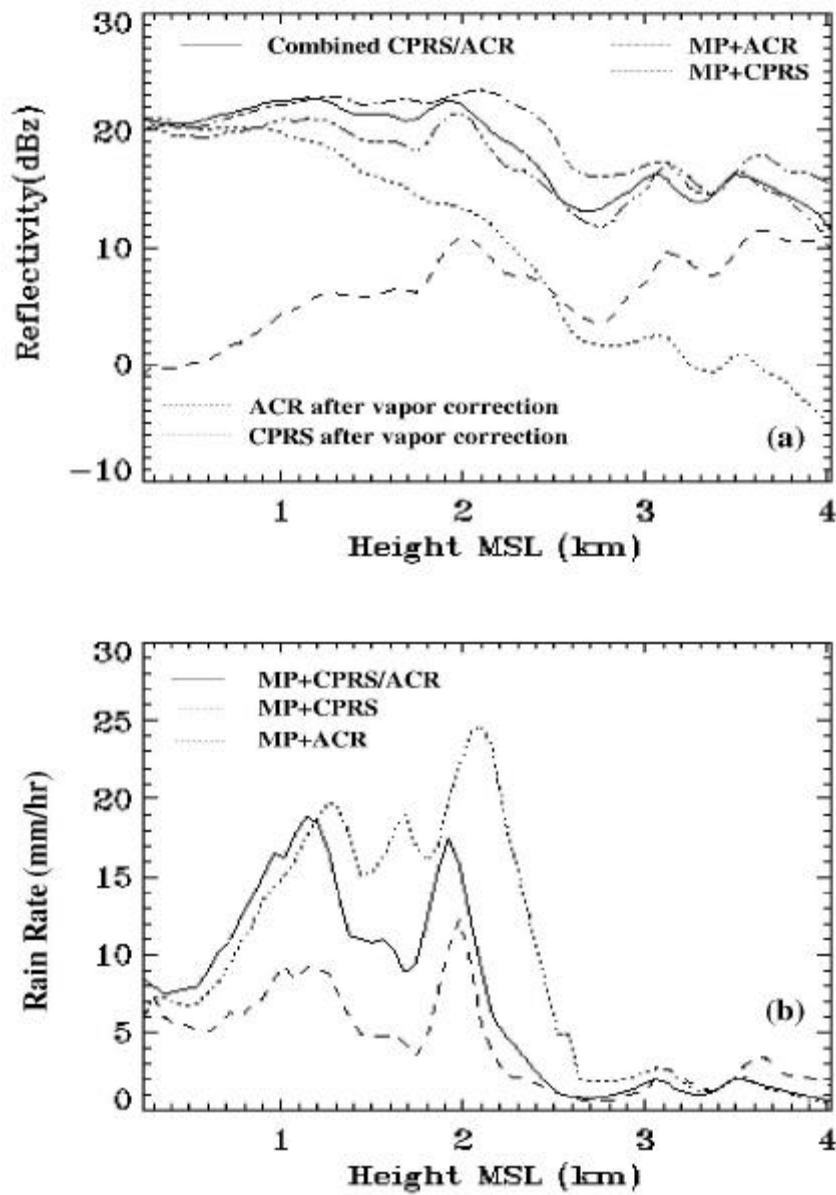


**Figure 3.** Reflectivity (a) and rain rate (b) retrieved by combining dual radar measurements and applying the HB algorithm to each individual radar profile. PIA was derived from the second radar data. The relations between  $Z_e^t$ ,  $K_p$  and  $R$  are derived from the Marshall-Palmer DSD.

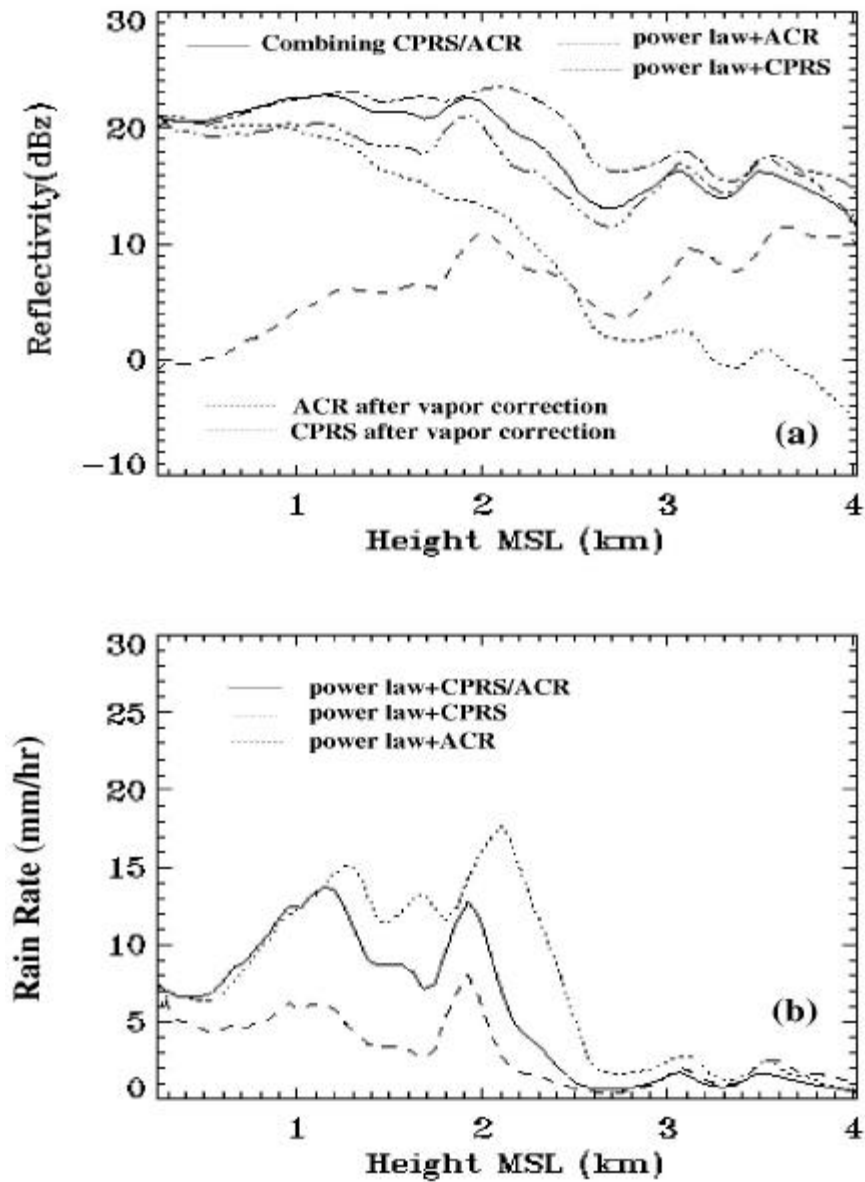


**Figure 4.** Reflectivity (a) and rain rate (b) retrieved by combining dual radar measurements and using the HB algorithm to each individual radar profile. PIA was derived from the second radar data. The relations between  $Z_e^t$ ,  $K_p$ , and R are given by  $Z_e^t = 30.0R^{0.71}$ , and  $K_p = 1.03 R^{0.8}$ .

Our second example illustrates analysis of the airborne radar measurements of precipitating clouds collected over the ocean. The HB algorithm and surface reference technique are used to retrieve reflectivity, attenuation and rain rate. Both of the profiles before and after atmospheric gas attenuation correction are shown in Figure 5. A 5.2-dB two-way PIA was obtained by comparing the ocean surface return from raining and rain-free area. Figure 6 plots the results using Marshall-Palmer DSD, different Gamma DSD (Ulbrich 1983) and power law relations.

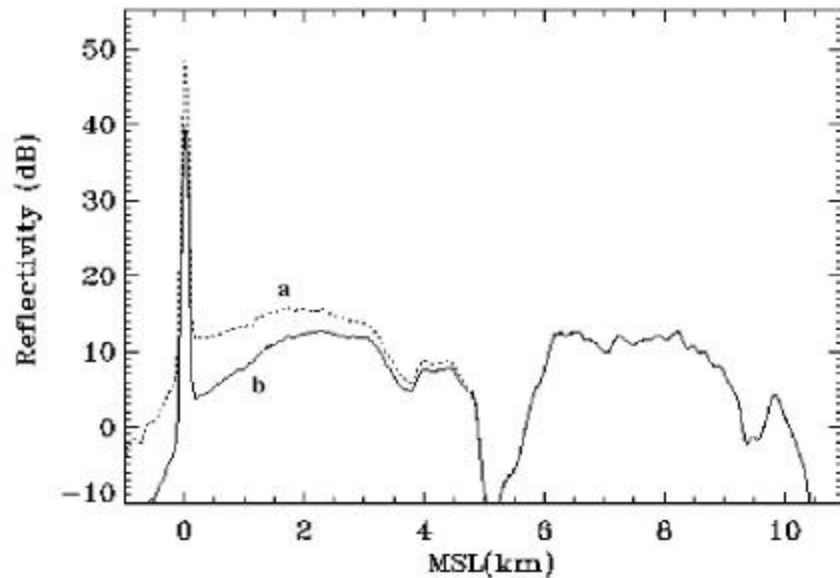


**Figure 5.** ACR reflectivity profiles of precipitation and cloud measured over the ocean. (a) after and (b) before the atmospheric gas attenuation correction.

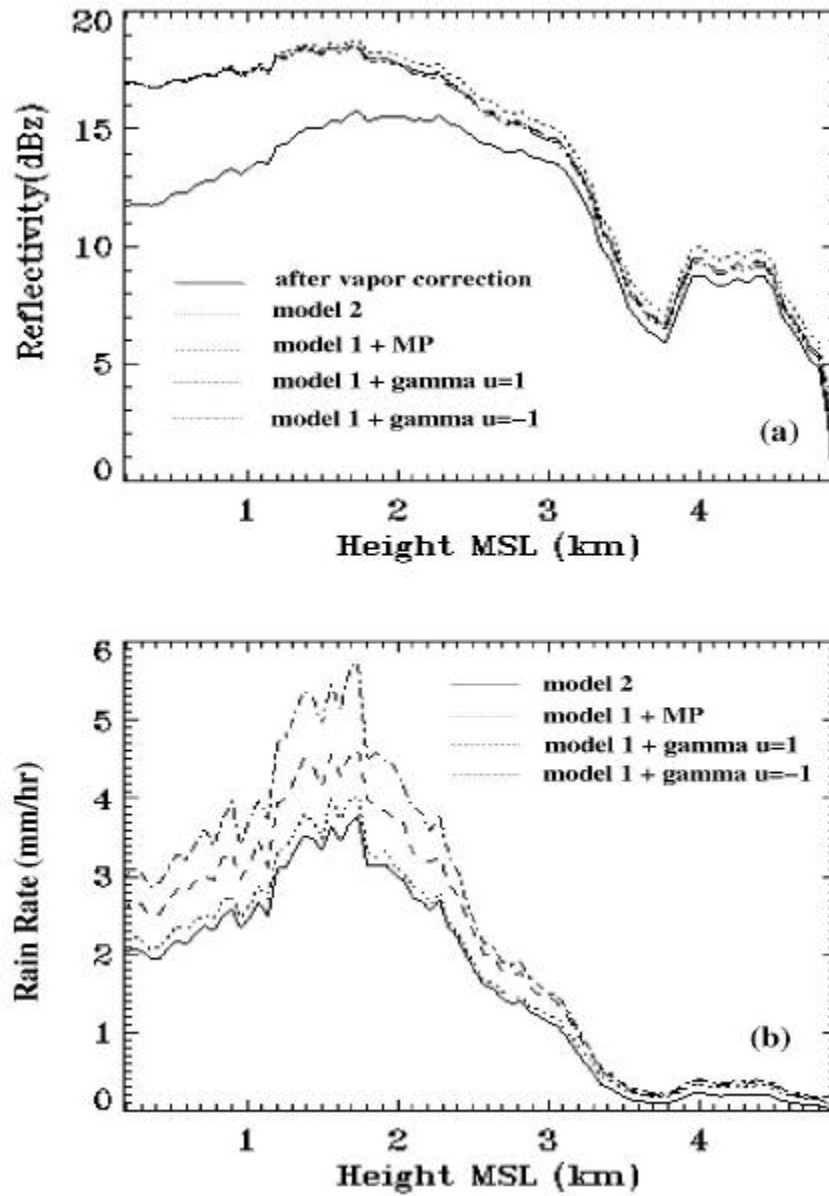


**Figure 6.** Reflectivity (a) and rain rate (b) estimated by using the HB algorithm. The relations between  $Z_e^t$ ,  $K_p$  and  $R$  are derived from different DSDs (Marshall-Palmer, Gamma) and from power law relations.

## References

- Doviak, R. J., and D. S. Zrnic, 1993: Doppler radar and weather observations. Academic Press, Inc.
- Haddad, Z. S., D. A. Short, S. L. Durden, E. Im, S. Hensley, M. B. Grable, and R. A. Black, 1997: A new parameterization of the rain drop size distribution. *IEEE Trans. Geo. Remote Sens.*, **35**, 532-539.
- Hitschfeld, W., and J. Bordan, 1954: Errors inherent in the radar measurements of rainfall at attenuating wavelengths. *J. Meteor.*, **11**, 58-67.
- Liebe, H. J., 1985: An updated model for millimeter-wave propagation in moist air. *Radio Sci.*, **5**(20), Sept.-Oct., 1069-1089.
- Meneghini, R., J. Eckerman, and D. Atlas, 1983: Determination of rain rate from a spaceborne radar using measurements of total attenuation. *IEEE Trans. Geo. Remote Sens.*, **21**, 34-43.
- Sadowy, G. A., R. E. McIntosh, S. J. Dindardo, S. L. Durden, W. N. Edelstein, F. K. Li, A. B. Tanner, W. J. Wilson, T. L. Schneider, and G. L. Stephens, 1997: The NASA DC-8 airborne cloud radar: Design and preliminary results. *International Geoscience and Remote Sensing Symposium*, Singapore.
- Sekelsky, S. M., L. Li, G. A. Sadowy, S. C. Reising, S. L. Durden, S. J. Dindardo, F. K. Li, A. C. Huffman III, and G. L. Stephens, 1999: Radar calibration validation for the SGP CART Summer 1998 DC-8 Cloud Radar Experiment. This proceedings.
- Ulbrich, C. W., 1983: Natural variations in the analytical form of the raindrop size distribution. *J. Climate and Appl. Meteor.*, **22**, 1764-1775.